

Nucleon-to-Resonance Electromagnetic Form Factors

Jorge Segovia

Nanjing University, and
Universidad Pablo de Olavide



11th Workshop on Hadron Physics in China and Opportunities Worldwide

Nankai University in Tianjin, China, August 23-28, 2019

A central goal of Nuclear Physics: understand the properties of hadrons in terms of the elementary excitations in Quantum Chromodynamics (QCD): quarks and gluons.

Transition form factors of nucleon resonances

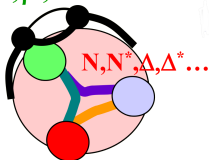
Unique window into their quark and gluon structure

Broad range of photon virtuality

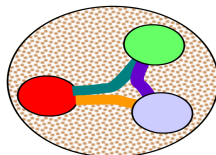
Distinctive information on the roles played by emergent phenomena in QCD

Probe the excited nucleon structures at perturbative and non-perturbative QCD scales

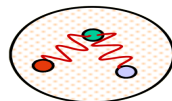
$\pi, \rho, \omega \dots$



3q-core+MB-cloud



3q-core



pQCD

Low Q^2

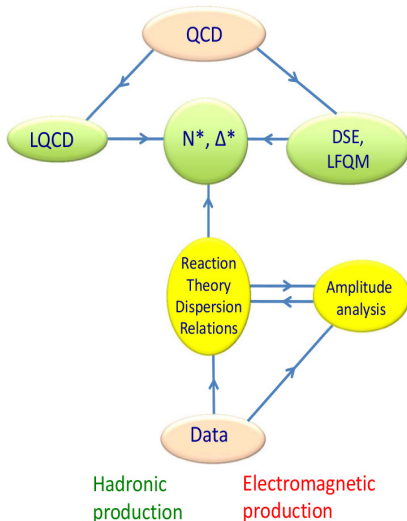
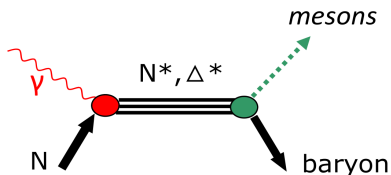
High Q^2

Studies of N^* photo- and electro-couplings (II)

*A vigorous experimental program has been and is still under way worldwide
CLAS, CBELSA, GRAAL, MAMI and LEPS*

- ☞ Multi-GeV polarized cw beam, large acceptance detectors, polarized proton/neutron targets.
- ☞ Very precise data for 2-body processes in wide kinematics (angle, energy): $\gamma p \rightarrow \pi N, \eta N, KY$.
- ☞ More complex reactions needed to access high mass states: $\pi\pi N, \pi\eta N, \omega N, \phi N, \dots$

Extract s-channel resonances



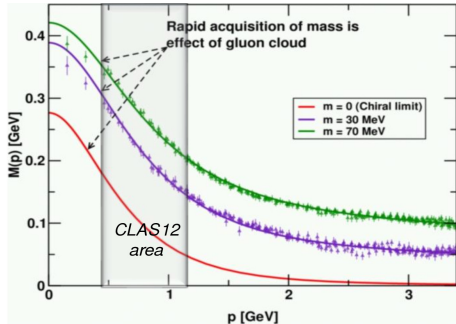
Upgrade of CLAS up to $12 \text{ GeV}^2 \rightarrow \text{CLAS12}$ (some experiments are underway)

CLAS obtained the most accurate results for the photo- and electro-excitation amplitudes:

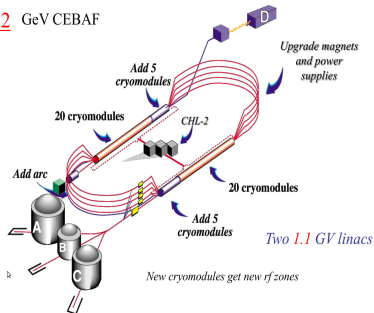
Up to 8.0 GeV^2 for $\Delta(1232)P_{33}$ and $N(1535)S_{11}$

Up to 4.5 GeV^2 for $N(1440)P_{11}$ and $N(1520)D_{13}$

CLAS12 will aim to measure the N^* photo- and electro-couplings at Q^2 ever achieved so far.



12 GeV CEBAF



We will be able to extract information about fundamental quantities in QCD

Emergence

Low-level rules producing high-level phenomena with enormous apparent complexity

Start from the QCD Lagrangian:

$$\mathcal{L}_{\text{QCD}} = -\frac{1}{4} G_a^{\mu\nu} G_{\mu\nu}^a + \frac{1}{2\xi} (\partial^\mu A_\mu^a)^2 + \partial^\mu \bar{c}^a \partial_\mu c^a + g f^{abc} (\partial^\mu \bar{c}^a) A_\mu^b c^c + \text{quarks}$$



Lattice, DSEs, ...

And obtain:

- ☞ Dynamical generation of fundamental mass scale in pure Yang-Mills (gluon mass).
- ☞ Quark constituent masses and chiral symmetry breaking.
- ☞ Bound state formation: mesons, baryons, glueballs, hybrids, multiquark systems...
- ☞ Signals of confinement.

Emergent phenomena could be associated with dramatic, dynamically driven changes in the analytic structure of QCD's Green's functions (propagators and vertices).

Quark propagator:

$$\text{---}\circ\text{---}^{-1} = \text{---}\text{---}^{-1} + \text{---}\overset{\text{gluon}}{\curvearrowright}\circ\text{---}$$

Ghost propagator:

$$\text{---}\circ\text{---}^{-1} = \text{---}\text{---}^{-1} + \text{---}\overset{\text{ghost}}{\curvearrowright}\circ\text{---}$$

Ghost-gluon vertex:

$$\text{---}\overset{\text{ghost}}{\curvearrowright}\circ\text{---} = \text{---}\overset{\text{ghost}}{\curvearrowright}\circ\text{---} + \text{---}\overset{\text{gluon}}{\curvearrowright}\overset{\text{ghost}}{\curvearrowright}\circ\text{---}$$

Quark-gluon vertex:

$$\text{---}\overset{\text{gluon}}{\curvearrowright}\circ\text{---} = \text{---}\overset{\text{gluon}}{\curvearrowright}\circ\text{---} + \text{---}\overset{\text{quark}}{\curvearrowright}\overset{\text{gluon}}{\curvearrowright}\circ\text{---} + \text{---}\overset{\text{gluon}}{\curvearrowright}\overset{\text{quark}}{\curvearrowright}\circ\text{---} + \text{---}\overset{\text{ghost}}{\curvearrowright}\overset{\text{gluon}}{\curvearrowright}\circ\text{---} + \text{---}\overset{\text{ghost}}{\curvearrowright}\overset{\text{ghost}}{\curvearrowright}\overset{\text{gluon}}{\curvearrowright}\circ\text{---} + \text{---}\overset{\text{quark}}{\curvearrowright}\overset{\text{ghost}}{\curvearrowright}\overset{\text{gluon}}{\curvearrowright}\circ\text{---} + \text{---}\overset{\text{gluon}}{\curvearrowright}\overset{\text{ghost}}{\curvearrowright}\overset{\text{gluon}}{\curvearrowright}\circ\text{---} + \text{---}\overset{\text{quark}}{\curvearrowright}\overset{\text{gluon}}{\curvearrowright}\overset{\text{ghost}}{\curvearrowright}\circ\text{---} + \text{---}\overset{\text{gluon}}{\curvearrowright}\overset{\text{quark}}{\curvearrowright}\overset{\text{ghost}}{\curvearrowright}\circ\text{---} + \text{---}\overset{\text{ghost}}{\curvearrowright}\overset{\text{quark}}{\curvearrowright}\overset{\text{gluon}}{\curvearrowright}\circ\text{---}$$

Gluon propagator:

$$\text{---}\overset{\text{gluon}}{\curvearrowright}\circ\text{---}^{-1} = \text{---}\text{---}^{-1} + \text{---}\overset{\text{quark}}{\curvearrowright}\overset{\text{gluon}}{\curvearrowright}\circ\text{---} + \text{---}\overset{\text{ghost}}{\curvearrowright}\overset{\text{gluon}}{\curvearrowright}\circ\text{---} + \text{---}\overset{\text{quark}}{\curvearrowright}\overset{\text{quark}}{\curvearrowright}\overset{\text{gluon}}{\curvearrowright}\circ\text{---} + \text{---}\overset{\text{ghost}}{\curvearrowright}\overset{\text{ghost}}{\curvearrowright}\overset{\text{gluon}}{\curvearrowright}\circ\text{---} + \text{---}\overset{\text{quark}}{\curvearrowright}\overset{\text{ghost}}{\curvearrowright}\overset{\text{gluon}}{\curvearrowright}\circ\text{---} + \text{---}\overset{\text{ghost}}{\curvearrowright}\overset{\text{quark}}{\curvearrowright}\overset{\text{gluon}}{\curvearrowright}\circ\text{---}$$

Off-shell Green's (correlation) functions

Even though they are:

- Gauge dependent.
- Renormalization point and scheme dependent.

However:

- They capture characteristic features of the underlying dynamics, both perturbative and non-perturbative.
- When appropriately combined they give rise to physical observables.

Theory tool based on Dyson-Schwinger equations

Interesting features:

- Inherently non-perturbative but, at the same time, captures the perturbative behavior \rightarrow accommodates the full range of physical momenta.
- Cover smoothly the full quark mass range, from the chiral limit to the heavy-quark domain.

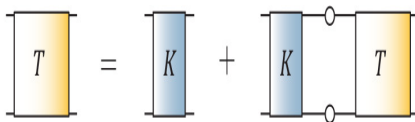
Main caveats:

- Truncation of the infinite system of coupled non-linear integral equations that preserves the underlying symmetries of the theory.
- No expansion parameter \rightarrow no formal way of estimating the size of the omitted terms \leftrightarrow the projection of higher Green's functions on the lower ones is small.

The bound-state problem in quantum field theory

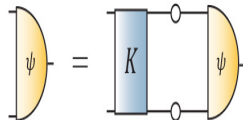
Extraction of hadron properties from poles in $q\bar{q}$, qqq , $qq\bar{q}\bar{q}$... scattering matrices

Use **scattering equation** (inhomogeneous BSE) to obtain T in the first place: $T = K + KG_0 T$



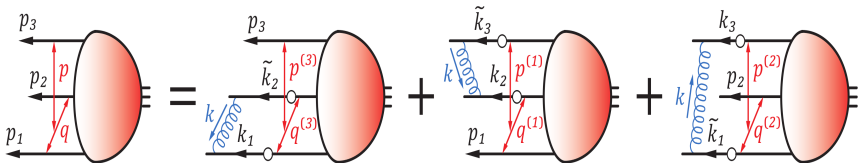
$p^2 \rightarrow -m^2$

Homogeneous BSE for **BS amplitude**:



☞ **Baryons**. A 3-body bound state problem in quantum field theory:

Faddeev equation in rainbow-ladder truncation

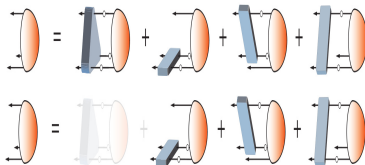


Faddeev equation: Sums all possible quantum field theoretical exchanges and interactions that can take place between the three dressed-quarks that define its valence quark content.

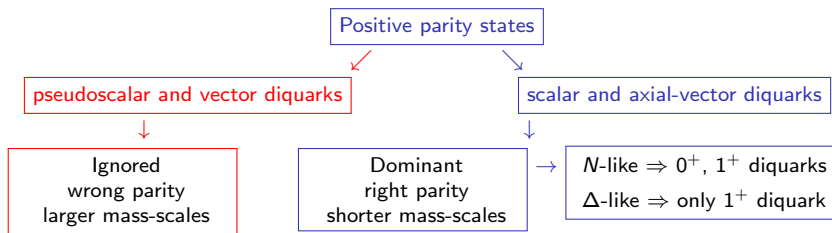
The attractive nature of quark-antiquark correlations in a colour-singlet meson is also attractive for $\bar{3}_c$ quark-quark correlations within a colour-singlet baryon

Diquark correlations:

- A tractable truncation of the Faddeev equation.
- In $N_c = 2$ QCD: diquarks can form colour singlets and are the baryons of the theory.
- In our approach: Non-pointlike colour-antitriplet and fully interacting.



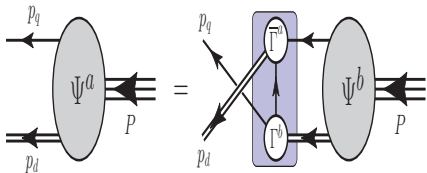
Diquark composition of the $N(940)$, $N(1440)$, $\Delta(1232)$ and $\Delta(1600)$



The quark+diquark structure of any baryon

☞ A baryon can be viewed as a **Borromean bound-state**, the binding within which has two contributions:

- Formation of tight diquark correlations.
- Quark exchange depicted in the shaded area.



☞ The exchange ensures that diquark correlations within the baryon are **fully dynamical**: no quark holds a special place.

☞ The rearrangement of the quarks guarantees that the baryon's wave function complies with **Pauli statistics**.

☞ Modern diquarks are **different from the old static, point-like diquarks** which featured in early attempts to explain the so-called missing resonance problem.

☞ The number of states in the **spectrum of baryons obtained is similar** to that found in the three-constituent quark model, just as it is in today's LQCD calculations.

☞ Modern diquarks enforce certain **distinct interaction patterns** for the singly- and doubly-represented valence-quarks within the baryon.

One-loop diagrams

Two-loop diagrams

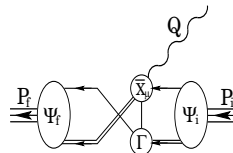
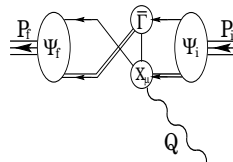
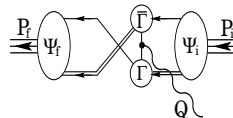
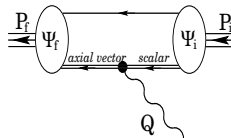
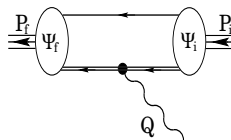
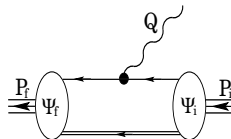
One must specify how the photon couples to baryon's constituents



Six contributions to the current in the quark-diquark picture



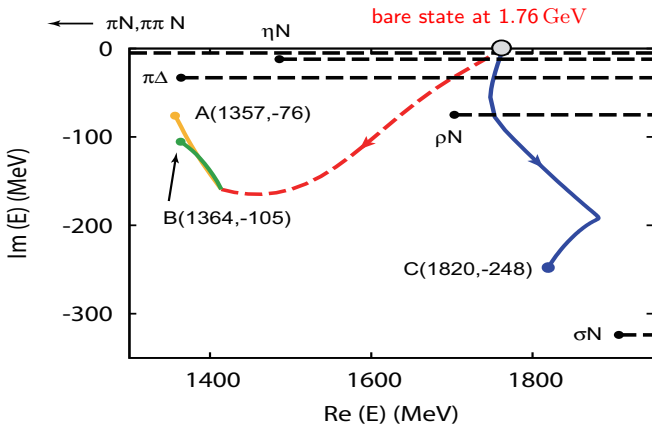
- Coupling of the photon to the dressed quark.
- Coupling of the photon to the dressed diquark:
 - ➔ Elastic transition.
 - ➔ Induced transition.
- Exchange and seagull terms.



$$\gamma^* N(940)\frac{1}{2}^+ \rightarrow N(1440)\frac{1}{2}^+$$

Based on:

- **Nucleon-to-Roper electromagnetic transition form factors at large Q^2**
C. Chen, Y. Lu, D. Binosi, C.D. Roberts, J. Rodríguez-Quintero, and J. Segovia
Phys. Rev. D99 (2019) 034013, arXiv:nucl-th/1811.08440
- **Structure of the nucleon's low-lying excitations**
C. Chen, B. El-Benich, C.D. Roberts, S.M. Schmidt, J. Segovia and S. Wan
Phys. Rev. D97 (2018) 034016, arXiv:nucl-th/1711.03142
- **Dissecting nucleon transition electromagnetic form factors**
J. Segovia and C.D. Roberts
Phys. Rev. C94 (2016) 042201(R), arXiv:nucl-th/1607.04405
- **Completing the picture of the Roper resonance**
J. Segovia, B. El-Bennich, E. Rojas, I.C. Cloët, C.D. Roberts, S.-S. Xu and H.-S. Zong
Phys. Rev. Lett. 115 (2015) 171801, arXiv:nucl-th/1504.04386

Disentangling the Dynamical Origin of P_{11} Nucleon ResonancesN. Suzuki,^{1,2} B. Juliá-Díaz,^{3,2} H. Kamano,² T.-S. H. Lee,^{2,4} A. Matsuyama,^{5,2} and T. Sato^{1,2}

The Roper is the proton's first radial excitation. *Its unexpectedly low mass arise from a dressed-quark core that is shielded by a meson-cloud which acts to diminish its mass.*

Nucleon's first radial excitation in DSEs

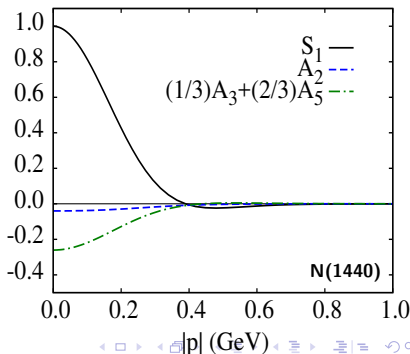
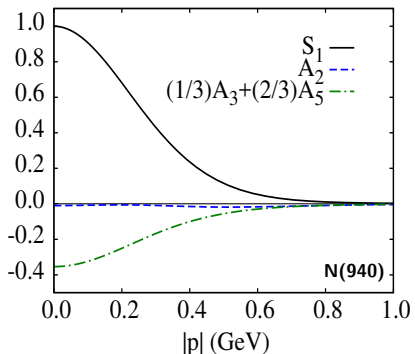
Bare-states of nucleon resonances correspond to hadron structure calculations which exclude the coupling with the meson-baryon final-state interactions

$$M_{Roper}^{DSE} = 1.73 \text{ GeV} \quad M_{Roper}^{EBAC} = 1.76 \text{ GeV}$$

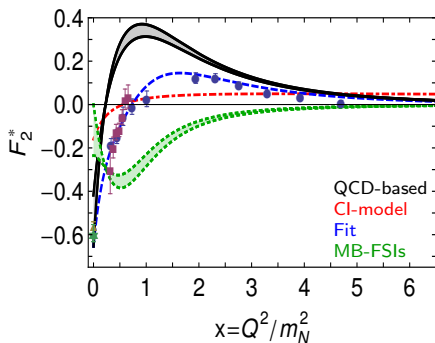
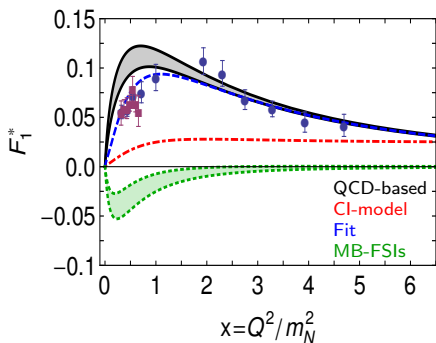
Observations:

- Meson-Baryon final state interactions reduce dressed-quark core mass by 20%.
- Roper and Nucleon have very similar wave functions and diquark content.
- A single zero in S-wave components of the wave function \Rightarrow A radial excitation.

0th Chebyshev moment of the S-wave components



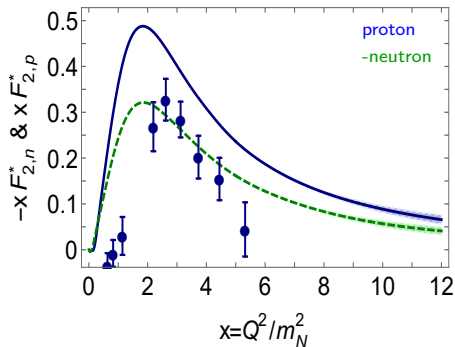
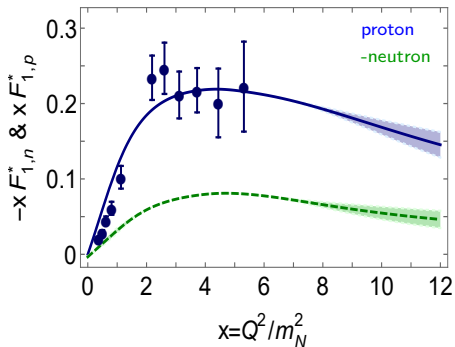
Nucleon-to-Roper transition form factors at high virtual photon momenta penetrate the meson-cloud and thereby illuminate the dressed-quark core



Observations:

- Our calculation agrees quantitatively in magnitude and qualitatively in trend with the data on $x \gtrsim 2$.
- The mismatch between our prediction and the data on $x \lesssim 2$ is due to meson cloud contribution.
- The dotted-green curve is an inferred form of meson cloud contribution from the fit to the data.

CLAS12 detector at JLab will deliver data on the Roper-resonance electroproduction form factors out to $Q^2 \sim 12m_N^2$ in both the charged and neutral channels



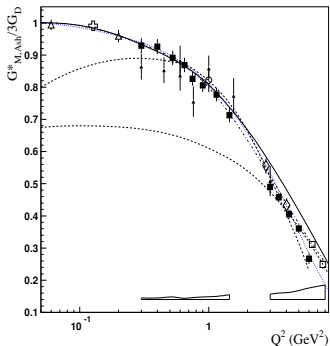
Observations:

- On the domain depicted, there is no indication of the scaling behavior expected of the transition form factors: $F_1^* \sim 1/x^2$, $F_2^* \sim 1/x^3$.
- Since each dressed-quark in the baryons must roughly share the momentum, Q , we expect that such behaviour will only become evident on $x \gtrsim 20$.

$$\gamma^* N(940) \frac{1}{2}^+ \rightarrow \Delta(1232) \frac{3}{2}^+$$

Based on:

- **Dissecting nucleon transition electromagnetic form factors**
J. Segovia and C.D. Roberts
Phys. Rev. C94 (2016) 042201(R), arXiv:nucl-th/1607.04405
- **Nucleon and Delta elastic and transition form factors**
J. Segovia, I.C. Cloët, C.D. Roberts and S.M. Schmidt
Few-Body Syst. 55 (2014) 1185-1222, arXiv:nucl-th/1408.2919
- **Elastic and transition form factors of the $\Delta(1232)$**
J. Segovia, C. Chen, I.C. Cloët, C.D. Roberts, S.M. Schmidt and S. Wan
Few-Body Syst. 55 (2014) 1-33, arXiv:nucl-th/1308.5225
- **Insights into the $\gamma^* N \rightarrow \Delta$ transition**
J. Segovia, C. Chen, C.D. Roberts and S. Wan
Phys. Rev. C88 (2013) 032201(R), arXiv:nucl-th/1305.0292

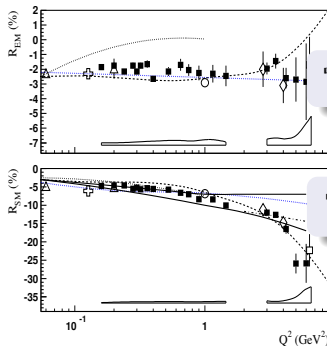


The $SU(6)$ predictions

(Symmetry considerations of baryon's wave function)

$$\langle p|\mu|\Delta^+ \rangle = \langle n|\mu|\Delta^0 \rangle$$

$$\langle p|\mu|\Delta^+ \rangle = -\sqrt{2} \langle n|\mu|n \rangle$$



The R_{EM} ratio is measured to be minus a few percent.

The R_{SM} ratio does not seem to settle to a constant at large Q^2 .

The CQM predictions

(Without quark orbital angular momentum)

$$R_{EM} = 0$$

$$R_{SM} = 0$$

The pQCD predictions

(Helicity arguments at very large photon's momenta)

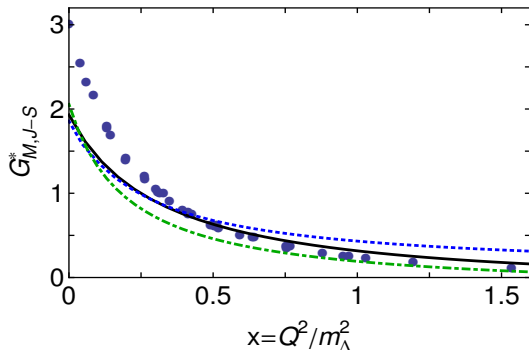
$$G_M^* \rightarrow 1/Q^4$$

$$R_{EM} \rightarrow 1$$

$$R_{SM} \rightarrow \text{constant}$$

Experimental data do not support theoretical predictions

$G_{M,J-S}^*$ cf. Experimental data and EBAC analysis



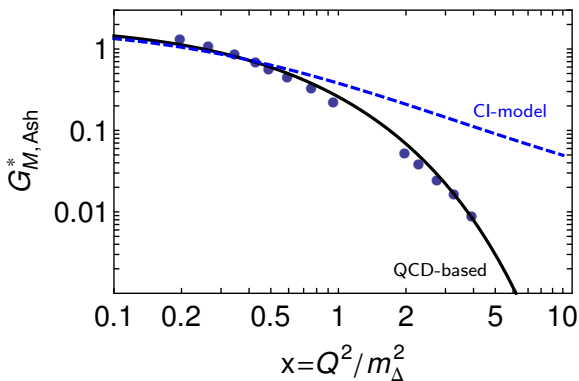
- Solid-black:
QCD-kindred interaction.
- Dashed-blue:
Contact interaction.
- Dot-Dashed-green:
Dynamical + no meson-cloud

Observations:

- All curves are in marked disagreement at infrared momenta.
- Similarity between Solid-black and Dot-Dashed-green.
- The discrepancy at infrared comes from omission of meson-cloud effects.
- Both curves are consistent with data for $Q^2 \gtrsim 0.75m_{\Delta}^2 \sim 1.14 \text{ GeV}^2$.

Presentations of experimental data typically use the Ash convention

– $G_{M,Ash}^*(Q^2)$ falls faster than a dipole –



☞ No sound reason to expect:

$$G_{M,Ash}^*/G_M \sim \text{constant}$$

☞ Jones-Scadron must exhibit:

$$G_{M,J-S}^*/G_M \sim \text{constant}$$

☞ Meson-cloud effects

- Up-to 35% for $Q^2 \lesssim 2.0m_{\Delta}^2$.
- Soft \rightarrow disappear rapidly.

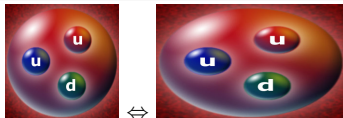
☞ $G_{M,Ash}^*$ vs $G_{M,J-S}^*$

- A Difference of $1/\sqrt{Q^2}$.

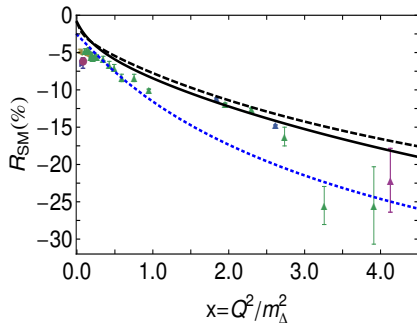
The electric- and coulomb-quadrupole ratios

☞ $R_{EM} = R_{SM} = 0$ in SU(6)-symmetric CQM.

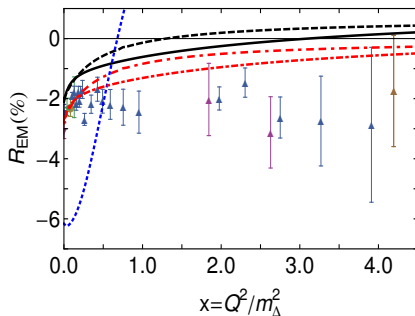
- Deformation of the hadrons involved.
- Modification of the transition current.



☞ R_{SM} : Good description of the rapid fall at large momentum transfer.



☞ R_{EM} : A particularly sensitive measure of orbital angular momentum correlations.



☞ *Zero Crossing in the electric transition form factor:*

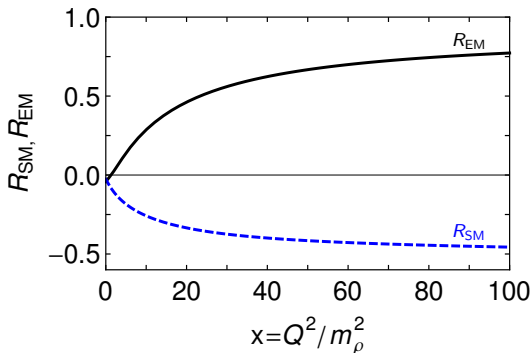
Contact interaction $\rightarrow Q^2 \sim 0.75m_\Delta^2 \sim 1.14 \text{ GeV}^2$

QCD-kindred interaction $\rightarrow Q^2 \sim 3.25m_\Delta^2 \sim 4.93 \text{ GeV}^2$

Helicity conservation arguments in pQCD should apply equally to:

- Results obtained within our QCD-kindred framework;
- Results produced by a symmetry-preserving treatment of a contact interaction.

$$R_{EM} \stackrel{Q^2 \rightarrow \infty}{\equiv} 1, \quad R_{SM} \stackrel{Q^2 \rightarrow \infty}{\equiv} \text{constant}.$$



Observations:

- Truly asymptotic Q^2 is required before predictions are realized.
- $R_{EM} = 0$ at an empirical accessible momentum and then $R_{EM} \rightarrow 1$.
- $R_{SM} \rightarrow \text{constant}$. Curve contains the logarithmic corrections expected in QCD.

$$\gamma^* N(940) \frac{1}{2}^+ \rightarrow \Delta(1600) \frac{3}{2}^+$$

Based on:

- **Transition form factors: $\gamma + p \rightarrow \Delta(1232), \Delta(1600)$**
Y. Lu, C. Chen, Z.-F. Cui, C.D. Roberts, S.M. Schmidt, J. Segovia, H.-S. Zong
Phys. Rev. D100 (2019) 034001, arXiv:nucl-th/1904.03205
- **Spec. and struc. of octet and decuplet and their positive-parity excitations**
C. Chen, G. Krein, C.D. Roberts, S.M. Schmidt and J. Segovia
Accepted by Phys. Rev. D, arXiv:nucl-th/1901.04305
- **Parity partners in the baryon resonance spectrum**
Y. Lu, C. Chen, C.D. Roberts, J. Segovia, S.-S. Xu and H.-S. Zong
Phys. Rev. C96 (2017) 015208, arXiv:nucl-th/1705.03988

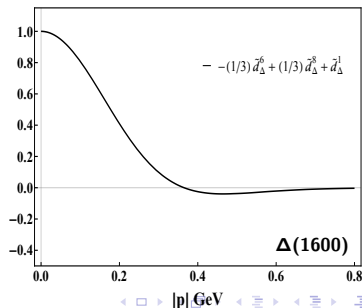
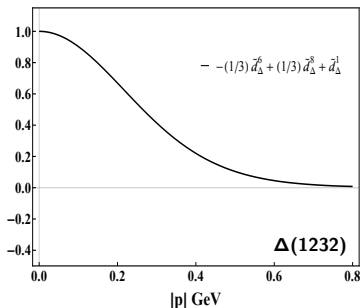
Bound-state kernels which omit meson-cloud corrections produce masses for hadrons that are larger than the empirical values (in GeV):

$$\begin{aligned}
 m_N &= 1.19 \pm 0.13, & m_\Delta &= 1.35 \pm 0.12, \\
 m_{N'} &= 1.73 \pm 0.10, & m_{\Delta'} &= 1.79 \pm 0.12.
 \end{aligned}$$

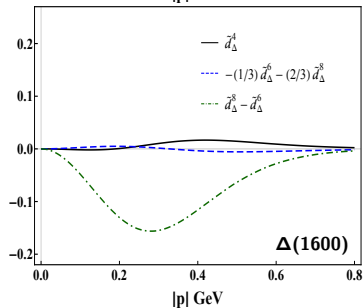
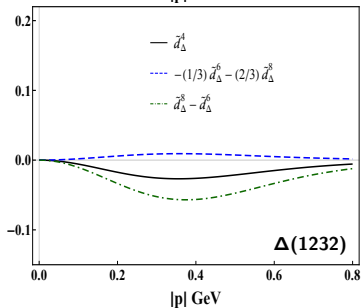
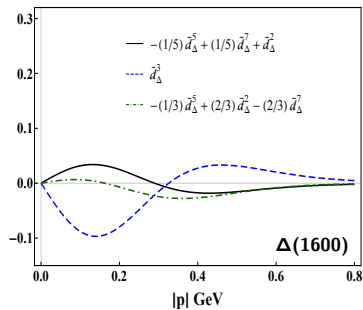
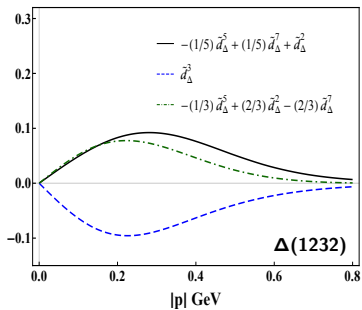
Observations:

- Meson-Baryon final state interactions reduce bare mass by 10 – 20%.
- The cloud's impact depends on the state's quantum numbers.
- A single zero in S-wave components of the wave function \Rightarrow A radial excitation.

0th Chebyshev moment of the S-wave component



Delta's first radial excitation in DSEs (II)



Wave function decomposition: $N(1440)$ cf. $\Delta(1600)$

	$N(940)$	$N(1440)$	$\Delta(1232)$	$\Delta(1600)$
scalar	62%	62%	—	—
pseudovector	29%	29%	100%	100%
mixed	9%	9%	—	—
<i>S</i> -wave	0.76	0.85	0.61	0.30
<i>P</i> -wave	0.23	0.14	0.22	0.15
<i>D</i> -wave	0.01	0.01	0.17	0.52
<i>F</i> -wave	—	—	~ 0	0.02

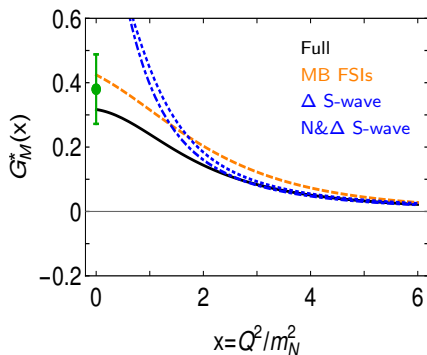
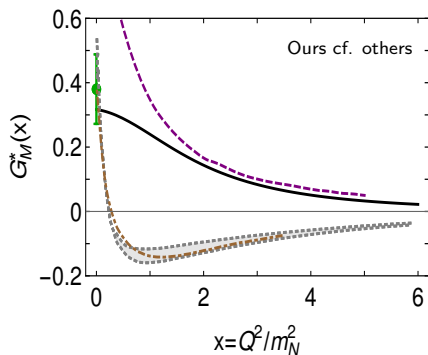
$N(1440)$

- Roper's diquark content are almost identical to the nucleon's one.
- It has an orbital angular momentum composition which is very similar to the one observed in the nucleon.

$\Delta(1600)$

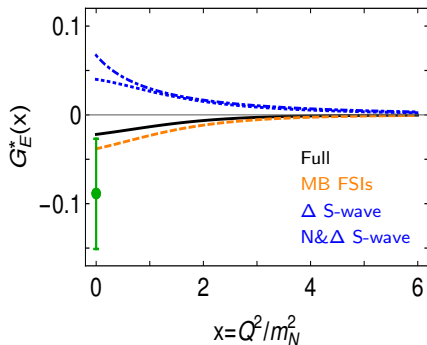
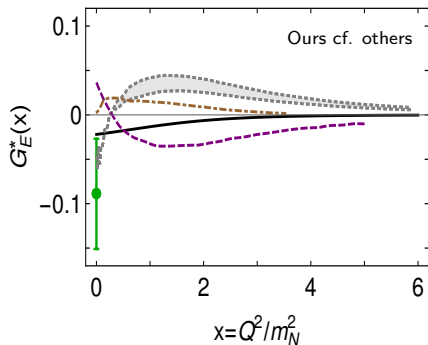
- $\Delta(1600)$'s diquark content are almost identical to the $\Delta(1232)$'s one.
- It shows a dominant $\ell = 2$ angular momentum component with its *S*-wave term being a factor 2 smaller.

The presence of all angular momentum components compatible with the baryon's total spin and parity is an inescapable consequence of solving a realistic Poincaré-covariant Faddeev equation



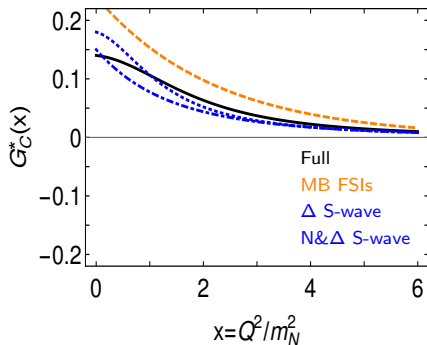
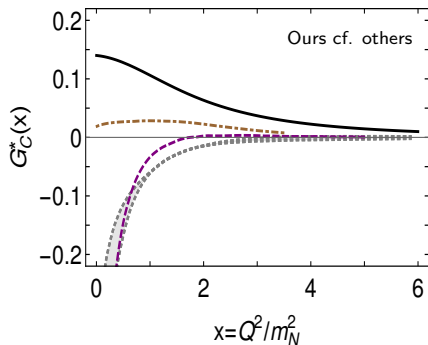
Observations:

- It is positive defined in the whole range of photon momentum and decreases smoothly with larger Q^2 -values.
- The mismatch with the empirical result are comparable with that in the $\Delta(1232)$ case, suggesting that MB FSIs are of similar importance in both channels.
- Higher partial-waves have a visible impact on G_M^* : They bring the magnetic dipole moment to lower values which could be compatible with experiment.



Observations:

- It is negative defined in the whole range of photon momentum and decreases smoothly with larger Q^2 -values.
- The mismatch with the empirical result could be due to meson cloud contributions.
- Higher partial-waves have a visible impact on G_E^* : They produce a change in sign which is crucial to get agreement with experiment at the real photon point.



Observations:

- It is positive defined in the whole range of photon momentum and decreases smoothly with larger Q^2 -values.
- Quark model results for all form factors are very sensitive to the wave functions employed for the initial and final states.
- MB FSIs could be important: a factor of two is observed for G_C^* at the real photon point. Moreover, higher partial-waves have a visible impact on G_C^* .

☞ The $\gamma^*N \rightarrow \text{Nucleon}' [\equiv N(1440)]$ reaction:

- Our calculation agrees quantitatively in magnitude and qualitatively in trend with the data on $x \gtrsim 2$. The mismatch on $x \lesssim 2$ is due to meson-cloud contribution.
- CLAS12@JLab will test our predictions for the charged and neutral channels in a range of momentum transfer larger than 4.5 GeV^2 .

☞ The $\gamma^*N \rightarrow \text{Delta} [\equiv \Delta(1232)]$ reaction:

- $G_{M,J-S}^{*p}$ falls asymptotically at the same rate as G_M^p . This is compatible with isospin symmetry and pQCD predictions.
- Data do not fall unexpectedly rapid once the kinematic relation between Jones-Scadron and Ash conventions is properly account for.
- Limits of pQCD, $R_{EM} \rightarrow 1$ and $R_{SM} \rightarrow \text{constant}$, are apparent in our calculation but truly asymptotic Q^2 is required before the predictions are realized.

☞ The $\gamma^*N \rightarrow \text{Delta}' [\equiv \Delta(1600)]$ reaction:

- G_M^* and R_{EM} are consistent with the empirical values at the real photon point, but we expect inclusion of MB FSIs to improve the agreement on $Q^2 \sim 0$
- R_{EM} is markedly different for $\Delta(1600)$ than for $\Delta(1232)$, highlighting the sensitivity of G_E^* to the degree of deformation of the Δ -baryons.
- R_{SM} is qualitatively similar for both $\gamma^*N \rightarrow \Delta(1600)$ and $\gamma^*N \rightarrow \Delta(1232)$ transitions, still larger (in absolute value) for the $\Delta(1600)$ case.

BACK SLIDES

Non-perturbative QCD: Dynamical generation of quark and gluon masses

☞ Dressed-quark propagator in Landau gauge:

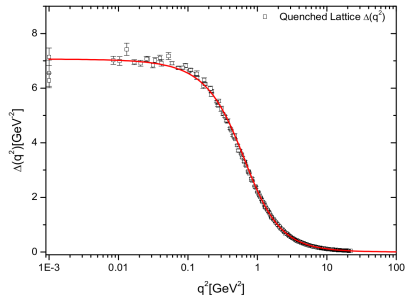
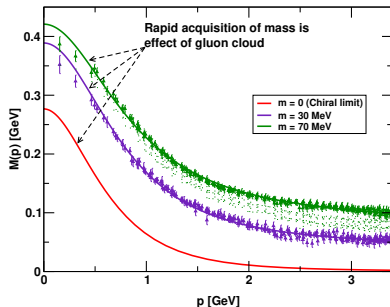
$$S^{-1}(p) = Z_2(i\gamma \cdot p + m) + \Sigma(p) = \left(\frac{Z(p^2)}{i\gamma \cdot p + M(p^2)} \right)^{-1}$$

- Mass generated from the interaction of quarks with the gluon-medium.
- Light quarks acquire a **HUGE** constituent mass.
- Responsible of the 98% of proton's mass, the large splitting between parity partners, ...

☞ Dressed-gluon propagator in Landau gauge:

$$i\Delta_{\mu\nu} = -iP_{\mu\nu}\Delta(q^2), \quad P_{\mu\nu} = g_{\mu\nu} - q_\mu q_\nu / q^2$$

- An inflexion point at $p^2 > 0$.
- Breaks the axiom of reflexion positivity.
- Gluon mass generation \leftrightarrow Schwinger mechanism.



Non-perturbative QCD: Ghost saturation and three-gluon-vertex suppression

☞ Dressed-ghost propagator in Landau gauge:

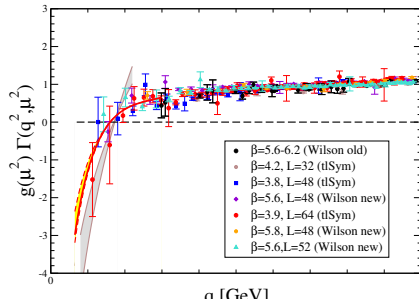
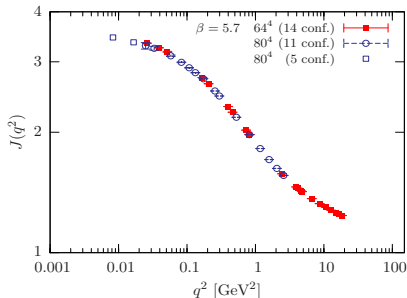
$$G^{ab}(q^2) = \delta^{ab} \frac{J(q^2)}{q^2}$$

- No power-like singular behavior at $q^2 \rightarrow 0$.
- Good indication that $J(q^2)$ reaches a plateau.
- Saturation of ghost's dressing function.

☞ Three-gluon vertex form factor in Landau gauge:
(\propto the tree-level tensor structure)

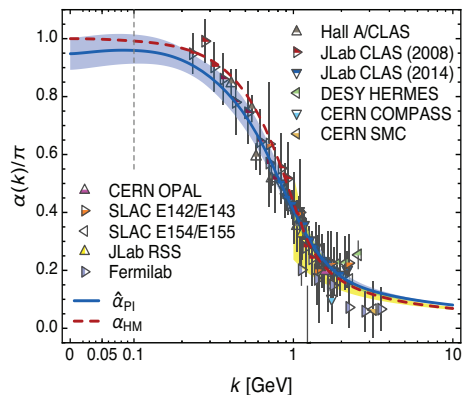
$$\Gamma_{T,R}^{\text{asym}}(q^2) \stackrel{q^2 \rightarrow 0}{\sim} F(0) \left[\frac{\partial}{\partial q^2} \Delta_R^{-1}(q^2) - C_1(r^2) \right]$$

- Appearance of (longitudinally coupled) massless poles.
- Suppression of the form factor in the so-called asymmetric momentum configuration.
- Plausible zero-crossing.



D. Binosi *et al.*, Phys. Rev. D96 (2017) 054026.

A. Deur *et al.*, Prog. Part. Nucl. Phys. 90 (2016) 1-74.



⊞ Perturbative regime:

$$\alpha_{g_1}(k^2) = \alpha_{\overline{\text{MS}}}(k^2) \left[1 + 1.14\alpha_{\overline{\text{MS}}}(k^2) + \dots \right]$$

$$\hat{\alpha}_{\text{PI}}(k^2) = \alpha_{\overline{\text{MS}}}(k^2) \left[1 + 1.09\alpha_{\overline{\text{MS}}}(k^2) + \dots \right]$$

⊞ Data = running coupling defined from the Bjorken sum-rule.

$$\int_0^1 dx \left[g_1^p(x, k^2) - g_1^n(x, k^2) \right] = \frac{g_A}{6} \left[1 - \frac{1}{\pi} \alpha_{g_1}(k^2) \right]$$

⊞ Curve determined from combined continuum and lattice analysis of QCD's gauge sector (massless ghost and massive gluon).

⊞ The curve is a running coupling that does NOT depend on the choice of observable.

- No parameters.
- No matching condition.
- No extrapolation.

⊞ It predicts and unifies an enormous body of empirical data via the matter-sector bound-state equations.

- **Go beyond RL truncation:**
implement dynamical symmetry breaking into bound-state equations

- **Same RL interaction strength Ansatz**

IR: Gaussian; UV: perturbative tail

[Qin, Chang, Liu, Roberts and Wilson, PRC 84 \(2011\)](#)

$$\mathcal{I}(k^2) = k^2 \frac{\mathcal{G}_{\text{IR}}(k^2) + \mathcal{G}_{\text{UV}}(k^2)}{4\pi}$$

$$\mathcal{G}_{\text{IR}}(k^2) = \frac{8\pi^2}{\omega^5} \zeta^3 e^{-k^2/\omega^2}$$

$$\mathcal{G}_{\text{UV}}(k^2) = \frac{96\pi^2}{25} \frac{1 - e^{-k^2/1[\text{GeV}^2]}}{k^2 \log[e^2 - 1 + (1 + k^2/\Lambda^2)^2]}$$

- **Quark-gluon vertex:**

$$\Gamma_\nu = \Gamma_\nu^{\text{BC}} + \Gamma_\nu^{\text{ACM}}$$

- **Ball-Chiu vertex**

completely determined by fermion propagator

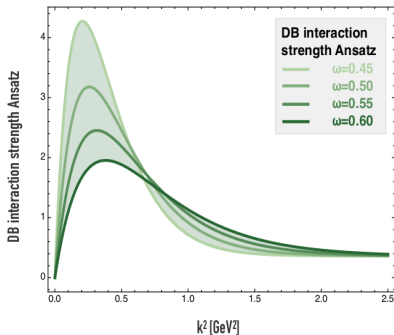
[Ball, Chiu PRD 22 \(1980\)](#)

- **Anomalous chromo-magnetic vertex**

transverse part (undetermined by STI)

- ζ fitted to

$$\zeta_{\text{DB}} = 0.55 [\text{GeV}]$$



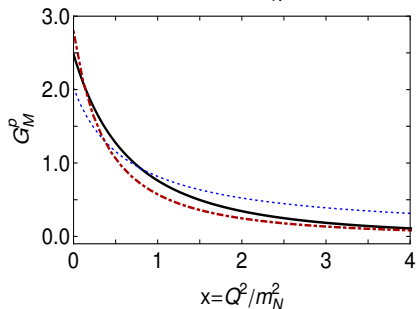
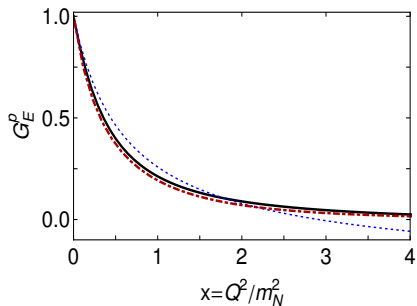
$$\gamma^* N(940) \frac{1}{2}^+ \rightarrow N(940) \frac{1}{2}^+$$

Based on:

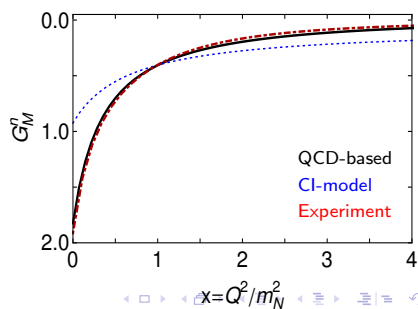
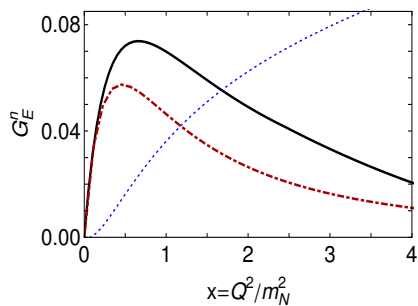
- **PDA: Revealing correlations within the proton and Roper**
C. Mezrag, J. Segovia, L. Chang and C.D. Roberts
Phys. Lett. B783 (2018) 263-267, arXiv:nucl-th/1711.09101
- **Contact-interaction Faddeev equation and, inter alia, proton tensor charges**
S.-S. Xu, C. Chen, I.C. Cloët, C.D. Roberts, J. Segovia and H.-S. Zong
Phys. Rev. D92 (2015) 114034, arXiv:nucl-th/1509.03311
- **Understanding the nucleon as a borromean bound-state**
J. Segovia, C.D. Roberts and S.M. Schmidt
Phys. Lett. B750 (2015) 100-106, arXiv:nucl-th/1506.05112
- **Nucleon and Delta elastic and transition form factors**
J. Segovia, I.C. Cloët, C.D. Roberts and S.M. Schmidt
Few-Body Syst. 55 (2014) 1185-1222, arXiv:nucl-th/1408.2919

Nucleon's electric and magnetic (Sachs) form factors

Q²-dependence of **proton** form factors:

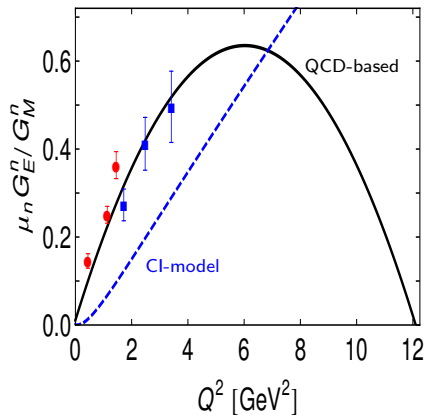
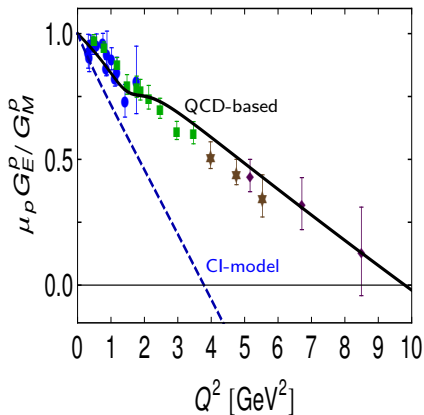


Q²-dependence of **neutron** form factors:



Unit-normalized ratio of Sachs electric and magnetic form factors (I)

Both CI and QCD-kindred frameworks predict a zero crossing in $\mu_p G_E^p / G_M^p$

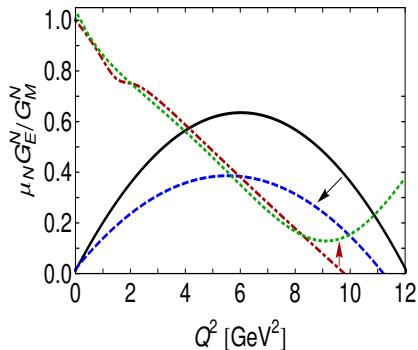
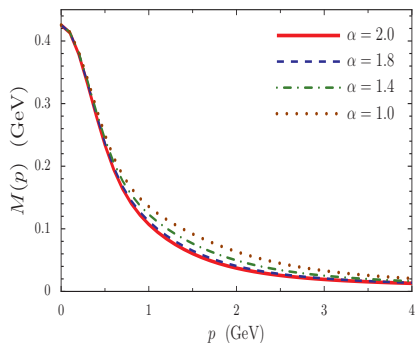


The possible existence and location of the zero in $\mu_p G_E^p / G_M^p$ is a fairly direct measure of the nature of the quark-quark interaction

Unit-normalized ratio of Sachs electric and magnetic form factors (II)

I. Cloët *et al.*, Phys.Rev.Lett. 111 (2013) 101803.

J. Segovia *et al.*, Few Body Syst. 55 (2014) 1185-1222.



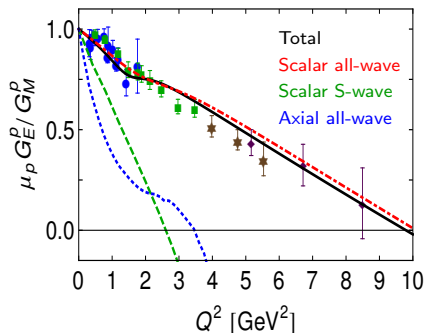
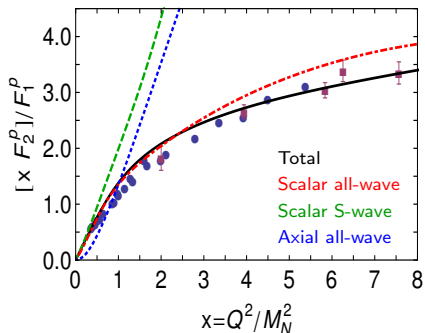
Black-solid and red-dot-dashed curves:

⇒ Unit-normalized ratio of Sachs electric and magnetic form factors of the neutron and proton, respectively.

Blue-dashed and green-dotted curves:

⇒ The same but using a momentum-dependent quark dressing with an accelerated rate of transition from dressed-quark → parton.

Implications of diquark correlations and Poincaré invariance



Observations:

- Axial-vector diquark contribution is not enough in order to explain the proton's electromagnetic ratios.
- Scalar diquark contribution is dominant and responsible of the Q^2 -behaviour of the the proton's electromagnetic ratios.
- Higher quark-diquark orbital angular momentum components of the nucleon are critical in explaining the data.

The presence of higher orbital angular momentum components in the nucleon is an inescapable consequence of solving a realistic Poincaré-covariant Faddeev equation

